

# DUCTILITY OF BIAXIALLY LOADED HIGH STRENGTH REINFORCED CONCRETE COLUMNS

AKRAM M. TORKEY<sup>1</sup> AND IBRAHIM G. SHAABAN<sup>2</sup>

## ABSTRACT

Eight reinforced High Strength Concrete "HSC" columns of dimensions 150 x 150 x 1200 mm were cast, tested and studied for both strength and deformational behavior. The investigated parameters included ratio of load eccentricity in both x and y directions, tie reinforcement ratio and configuration, and vertical steel percentage. Within the limits of the test results of this study, it was found that increasing load eccentricity resulted in reducing the ultimate capacity of the studied HSC columns by approximately 15%. In addition, increasing the lateral confinement lead to an increase of ultimate capacity by approximately 22%. Moreover, tie configuration was more effective than ties reinforcement ratio on the ductility of studied HSC columns. Increasing vertical steel percentage lead to an improvement of ductility of HSC columns. A proposed design formula was developed for predicting the capacity of eccentric and biaxially loaded HSC columns.

**KEYWORDS:** high-strength concrete; reinforced concrete; columns; ductility; eccentric loading; displacement; design procedures.

## 1. INTRODUCTION

Over the last fifteen years, improvements in material technology and in the production of ready mixed concrete have resulted in the availability of higher concrete strength grades [1]. A number of projects in the United States, Europe, Australia, and Japan have been completed using such concrete [2]. The use of High Strength Concrete (HSC) is now common practice in reinforced concrete structural elements especially heavily loaded columns. During the last few years, extensive experimental and

---

<sup>1</sup>Associate Professor, Structural Engineering Department, Cairo University

<sup>2</sup>Associate Professor, Civil Engineering Department, Zagazig University "Banha Branch"

analytical work have provided a better understanding of the behavior of HSC axially and eccentrically loaded columns [3]. However, most design codes include proportioning equations of empirical constants based on tests using Normal-Strength Concrete (NSC) [3]. It is worth mentioning that columns constructed from HSC and designed using the same tie strengths and spacing as conventional strength concrete columns are more brittle and have less ductility [1].

Reinforced concrete columns in moment-resisting space frames constructed in areas of high seismicity are subjected to compression with uniaxial or biaxial bending. Such columns should be proportioned to have adequate curvature and displacement properties in order to be capable of behaving inelastically without appreciably losing load-carrying capacity [4]. The spacing, amount and configuration of lateral reinforcement influences the confinement provided to the column core. Providing the code minimum tie reinforcement in conventional strength concrete columns allows for some ductility for columns under applied loads. It is important to estimate the difference in the safety margin between structures using conventional strength concretes designed to current codes of practice and their HSC alternatives [1]. There are many investigations in the literature to study the behavior of HSC columns [5, 6 and 7]. However, very limited studies were cited in the literature on the behavior of HSC columns subject to both axial load and biaxial bending.

This paper presents the experimental results from the testing of seven HSC columns of strength  $800 \text{ kg/cm}^2$  and a control NSC column of strength  $300 \text{ kg/cm}^2$ . The studied parameters were the amount of longitudinal and lateral reinforcement, ties ratio and configuration, and different ranges of eccentricities at both x and y directions. The ultimate strength results and ductility measures are presented for different studied parameters. The results were predicted using available design charts. A proposed design empirical formula was developed and used in predicting the results.

## 2. EXPERIMENTAL PROGRAM

In this research all specimens were tested and studied under the action of compression force combined with biaxial bending concerning both strength and behavior. Different parameters such as eccentricities, percentage of reinforcement and shape of ties were considered. All columns were square in shape of height " $h$ " = 120 cm and width " $b$ " = 15 cm to achieve height to width ratio " $h/b$ " = 8 to avoid buckling.

### 2.1 Test Specimens

Eight columns were tested under the action of normal force with biaxial bending. Concrete strains and lateral deformations were measured. Figure 1 and Table 1 show the description of the columns along with the studied parameters.

### 2.2 Materials

The steel used for the longitudinal reinforcement consisted of eight 10 mm diameter high grade steel except for Specimen No. 8 of 12 mm diameter. This gave longitudinal steel reinforcement ratios of 2.8 and 4 percent, respectively. The characteristic yield strength for steel used is 3600 kg/cm<sup>2</sup>. Column tie reinforcement was fabricated from 6 mm mild steel round bars of characteristic strength 2400 kg/cm<sup>2</sup>. The tie reinforcement was spaced at 80 mm except for Specimen No. 5 was spaced at 50 mm as described in Table 1. Three tie configurations were used in this study as shown in Figure 1.

Two different mixes were used to develop normal and high strength concrete at 28 days of target strength 300 and 800 kg/cm<sup>2</sup>, respectively. The actual cube compressive strengths for different specimens are given in Table 1. Table 2 provides the mix designs for the two concrete strengths. Sand and coarse aggregate (basalt) used were from a local pit. Two different size distributions of the basalt (14 and 5mm) were blended to obtain a uniform distribution. A superplasticizer based on polynaphthalene sulphate was used to improve the workability of the concrete mix. Ten percent by weight of the portland cement was replaced by silica fume to produce

concrete of target strength  $800 \text{ kg/cm}^2$ . The specimens were cast in wooden forms and standard cubes were prepared to check the strength of the specimens. The column specimens and standard cubes were cured in water bath for a minimum 28 days. Cube compression tests were conducted in accordance with E.C. 95 Clause (8-6-7-3) [8].

Table 1 Description of the Studied Column Specimens

Column Specimen Number	Concrete Strength ( $\text{kg/cm}^2$ )	Reinforcement			Load Eccentricity	
		Longitudinal <sup>•</sup>	Transverse		$e_x$ (cm)	$e_y$ (cm)
			amount	Type		
C1	748	8 $\Phi$ 10	$\phi$ 6 @ 8cm	A	2.25	2.25
C2	762	8 $\Phi$ 10	$\phi$ 6 @ 8cm	A	4.50	4.50
C3	735	8 $\Phi$ 10	$\phi$ 6 @ 8cm	A	4.50	2.25
C4*	386	8 $\Phi$ 10	$\phi$ 6 @ 8cm	A	2.25	2.25
C5	782	8 $\Phi$ 10	$\phi$ 6 @ 5cm	A	2.25	2.25
C6	782	8 $\Phi$ 10	$\phi$ 6 @ 8cm	B	2.25	2.25
C7	790	8 $\Phi$ 10	$\phi$ 6 @ 8cm	C	2.25	2.25
C8	734	8 $\Phi$ 12	$\phi$ 6 @ 8cm	A	2.25	2.25

\* Normal Strength Concrete "NSC" column.

•  $\Phi$  denotes high grade steel with  $3600 \text{ kg/cm}^2$ , yield stress.

Table 2 Mix Designs of Medium and High Strength Concrete

Characteristic Strength	Constituents and Mix proportions, $\text{kg/m}^3$					
	Cement	Sand	Crushed Basalt	Water	Silica Fume	Superplasticizer
Mix 1, $300 \text{ kg/cm}^2$	350	650	1150	160	---	4
Mix 2, $800 \text{ kg/cm}^2$	575	623	957	142	70	20

### **2.3 Instrumentation and Testing Procedure**

A 500-ton capacity test machine capable of testing columns up to 6 m height was used for testing the columns. It consists of lower moving piston, which moves on a spherical head covered by a plate so that the applied load is always passing through the center of the sphere and perpendicular to the column cross-section whenever the eccentricity is applied. The upper plate is capable of moving around a fixed sphere. A schematic diagram for the test machine is shown in Figure 2. The readings were taken on a calibrated mechanical dial. The load was applied through a steel plate 5 x 5 x 2 cm placed on the top of the column (see Figure 1) at the required eccentricity reported in Table 1 while the base of the column was placed directly on the lower plate. Steel straps were used on the top 15 cm of the column to minimize the stress concentration which can result from applying the load to the small steel plate in order to obtain the required eccentricity [9] (see Figures 1 and 3).

### **2.4 Rate of loading**

Each column was located in the test machine. The initial reading of all demec strain gauge dials were taken before the beginning of the test. The load was incrementally applied with an increment rate of 10 ton/step for all specimens except Specimen No. 4 of normal strength concrete in which the load was applied at a rate of 5 ton/step. Before failure, the rate was reduced to one half of the aforementioned loading rates. At each stage of loading, cracks were observed and marked, if any. The readings of all dials were recorded in order to calculate strains and lateral deformations in concrete.

### **2.5 Concrete strain and lateral deformation devices**

Concrete strains were measured by a 150 mm demec gauge, for better accuracy. Lateral column deformations were measured at each stage of loading by two dial gauges (of 0.001 mm accuracy) on each side of the column. The gauges were placed apart from the mechanical strain gauge locations at two different places as shown in Figure 1.



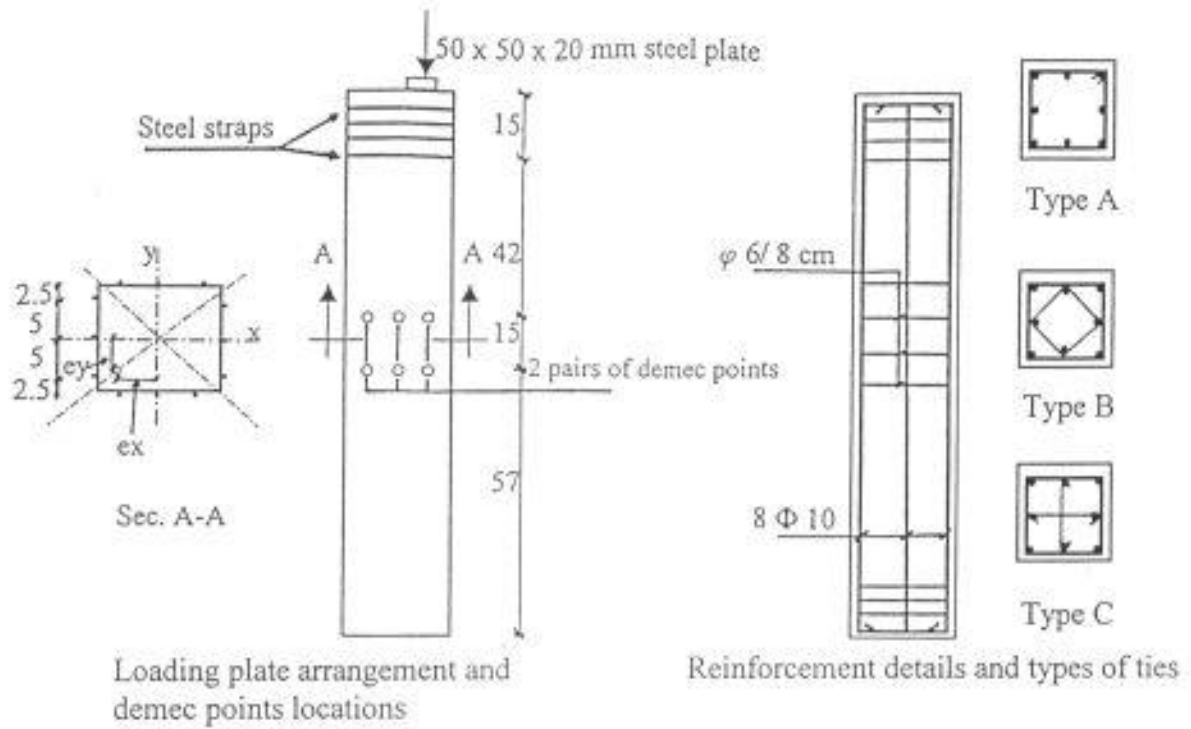


Figure 1 Typical column dimensions, steel reinforcement and measurement locations.

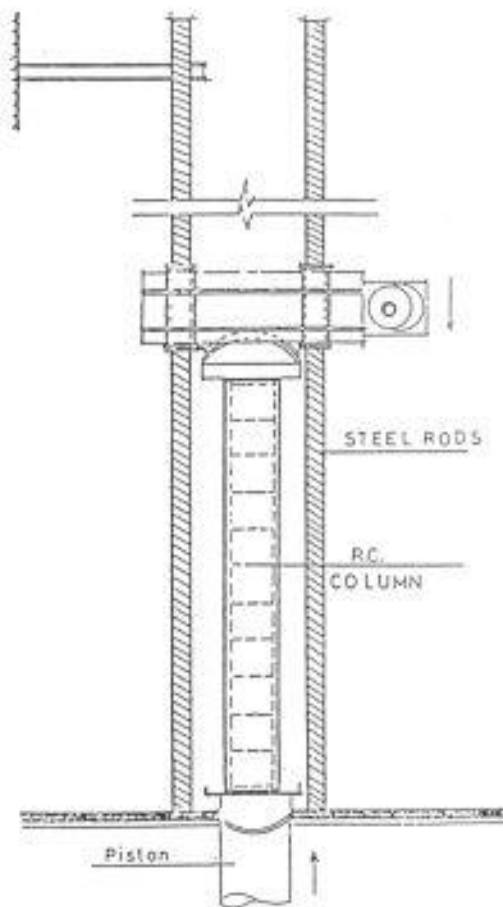


Figure 2 The testing machine.

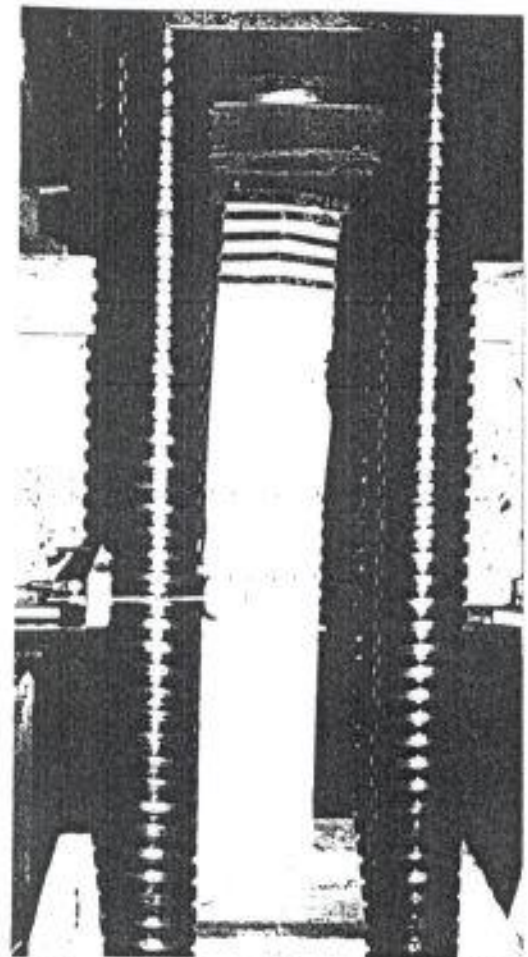


Figure 3 A typical column during testing.

### 3. ANALYTICAL STUDY

#### 3.1 Interaction Diagrams

The design of columns subjected to biaxial bending using interaction diagrams is the easiest method for designing such columns. An analytical investigation was carried out using the computer model developed earlier [10] and modified for application on HSC columns. The model is based on the strain compatibility and complies with E.C. 95 [8]. It performs the integration of the stress diagram over the column cross section to obtain the complete interaction diagram or the failure surface in the biaxial case (the original form is an onion shape). A sample of the output charts for the case of " $e_x$ " equals " $e_y$ " is presented in Figure 4.

#### 3.2 Proposed Design Approach

A reduction factor " $K$ " was introduced earlier [11], on the ultimate strength of high strength concrete columns to estimate the ultimate load of these columns as follows:

$$K = 0.6 + 12.5 / f_{cu} \quad (1)$$

And the ultimate strength of normal strength concrete columns is:

$$P_n = 0.67 f_{cu} (A_g - A_s) + A_s f_y \quad (2)$$

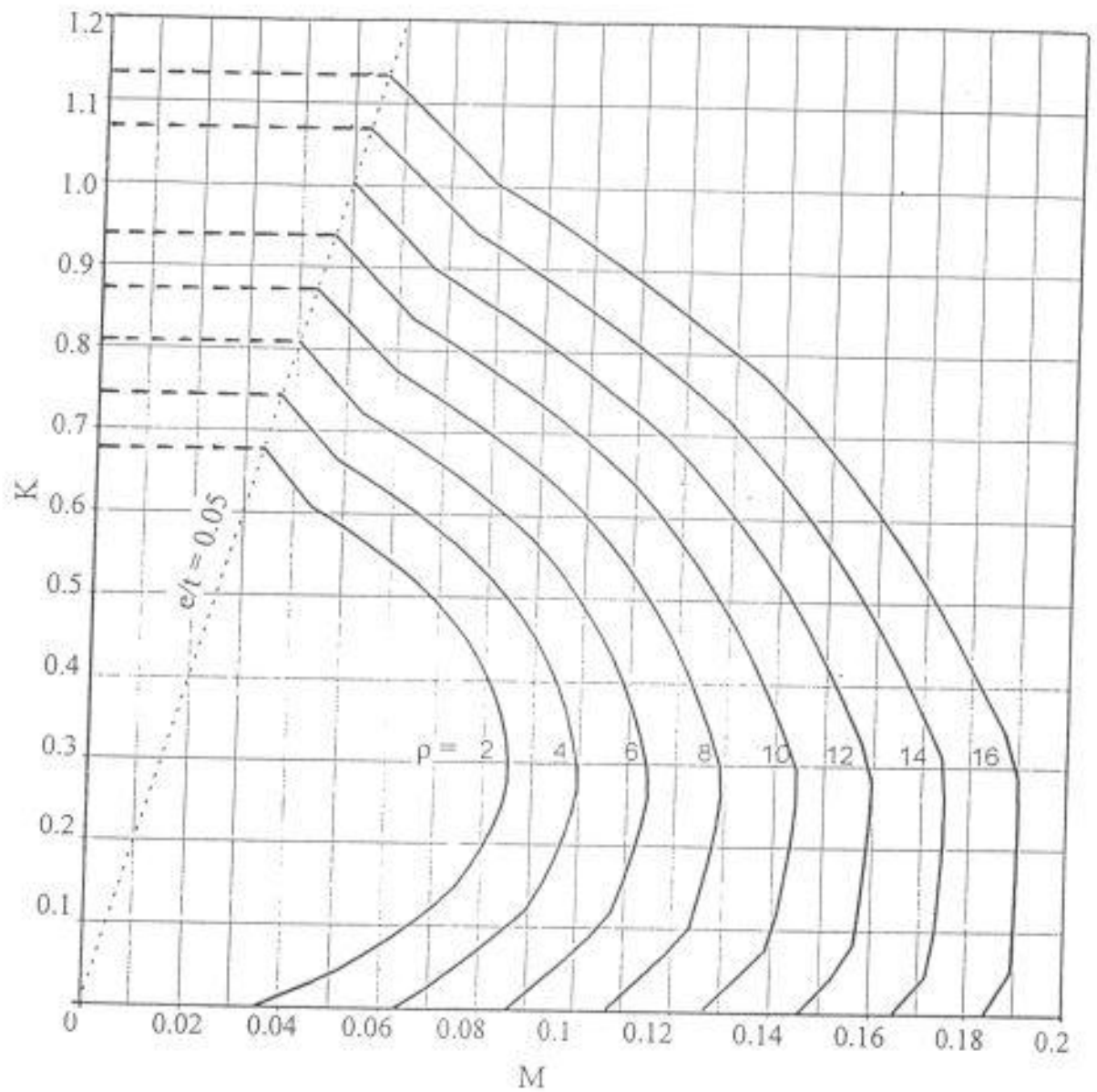
The ultimate strength of HSC columns " $P_{max}$ " is estimated as:

$$P_{max} = K P_n \quad (3)$$

Where:

- $f_{cu}$  = concrete compressive strength, MPa
- $A_g$  = gross area of column section, mm<sup>2</sup>
- $A_s$  = area of steel reinforcement, mm<sup>2</sup>
- $f_y$  = longitudinal reinforcement yield stress, MPa

However, the introduced factor " $K$ " did not consider the effect of the eccentricity ratio and confinement effect. Liu et. al. [12] proposed a confinement effectiveness parameter " $K_c$ " for HSC concentrically loaded columns which is based on a model developed earlier by Sheikh and Uzmeri [13]:



$$M = \sqrt{(M_x / f_{cu} b t^2)^2 + (M_y / f_{cu} t b^2)^2}$$

$$K = P_u / f_{cu} b t$$

$$\mu = \rho f_{cu} 10^{-5}$$

$$A_s (\text{total}) = \mu b t$$

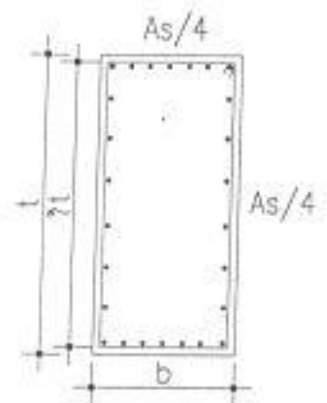


Figure 4 Interaction diagram for biaxially loaded columns [10].



$$K_c = \left( 1 - \frac{1}{6 A_{core}} \sum_{i=1}^n W_i^2 \right) \left( 1 - \frac{S^*}{2 b_c} \right) \left( 1 - \frac{S^*}{2 d_c} \right) \quad (4)$$

Where:

$W_i$  =  $i$ th clear distance between adjacent tied longitudinal bars;

$n$  = number of spaces between the tied longitudinal bars;

$b_c$  and  $d_c$  = core dimensions to the centerline of the ties across the width and depth of the section;

$A_{core} = b_c d_c$ ; and

$S^*$  = clear spacing between the ties, as used by Mander et al. [14].

Equation (4) is modified in order to be applied for studied square columns;

$$K_c = \left( 1 - \frac{1}{6 A_{core}} \sum_{i=1}^n W_i^2 \right) \left( 1 - \frac{S^*}{2 b_c} \right)^2 \quad (5)$$

A factor including the effect of eccentricity " $K_e$ ", based on the applied eccentricities and columns' dimensions is developed in this investigation;

$$K_e = 1.0 - \frac{e}{4 b_c} \quad (6)$$

Where:

$$e = \sqrt{[(e_x)^2 + (e_y)^2]}$$

$e_x, e_y$  = load eccentricity in x and y directions.

The ultimate load of high strength concrete columns under biaxial eccentric loads is estimated in Equation (7) by substituting Equations (5) and (6) into Equation (3) as follows:

$$P_{max} = K K_e (0.5 + K_c) P_n \quad (7)$$

## 4. RESULTS AND DISCUSSION

### 4.1 Experimental Results

#### 4.1.1 Crack Pattern and Failure Mode

Figure 5 shows crack patterns for different studied column specimens. Normal strength short column specimen "C4" under initial eccentricities " $e_x$ " and " $e_y$ " = 2.25 cm (eccentricity ratio,  $e/t = 0.21$ ) showed a typical tension failure pattern. Flexural cracks formed at low load levels and gradually developed as the load increased. Failure load was reached when the tensile face was fully cracked at mid-height of the column, and the extreme compressive fiber crushed. It can be seen from Figure 5 that a different column failure mode exists with HSC columns. While concrete crushing (due to failure either in compression face or in tension face) was observed at the extreme fiber of the NSC column "C4", HSC column specimens failed by compressive cover spalling regardless of the initial eccentricities. Similar observations were found by Lee and Son [6].

It can be seen from Figure 5 that the tensile cracks are uniformly distributed all over the height of the columns "C1", "C2", "C3", "C5", and "C7". However, the number of cracks increases with the increase of eccentricities " $e_x$ " and " $e_y$ " as observed for columns "C2" and "C3" compared to Column "C1". In addition, the number of cracks decreased with the increase of longitudinal reinforcement as observed in Column "C8". It is interesting to notice that increasing the number of stirrups as shown in Column "C5" did not affect the number of cracks. Columns "C2" and "C5" and "C8" showed a failure of concrete core near the ultimate load and after the failure of the steel straps on the top of the column. Column "C3" shows a failure of concrete in compression near to the base as a result of the rotation of the spherical head of the testing machine. Column "C6" was separated into two parts and the cracks were wider prior to failure. It was observed that Column "C7" failed in compression by crushing of the concrete core together with buckling of the longitudinal reinforcement at the corner. This is similar to the observations of Liu et. al. [12].

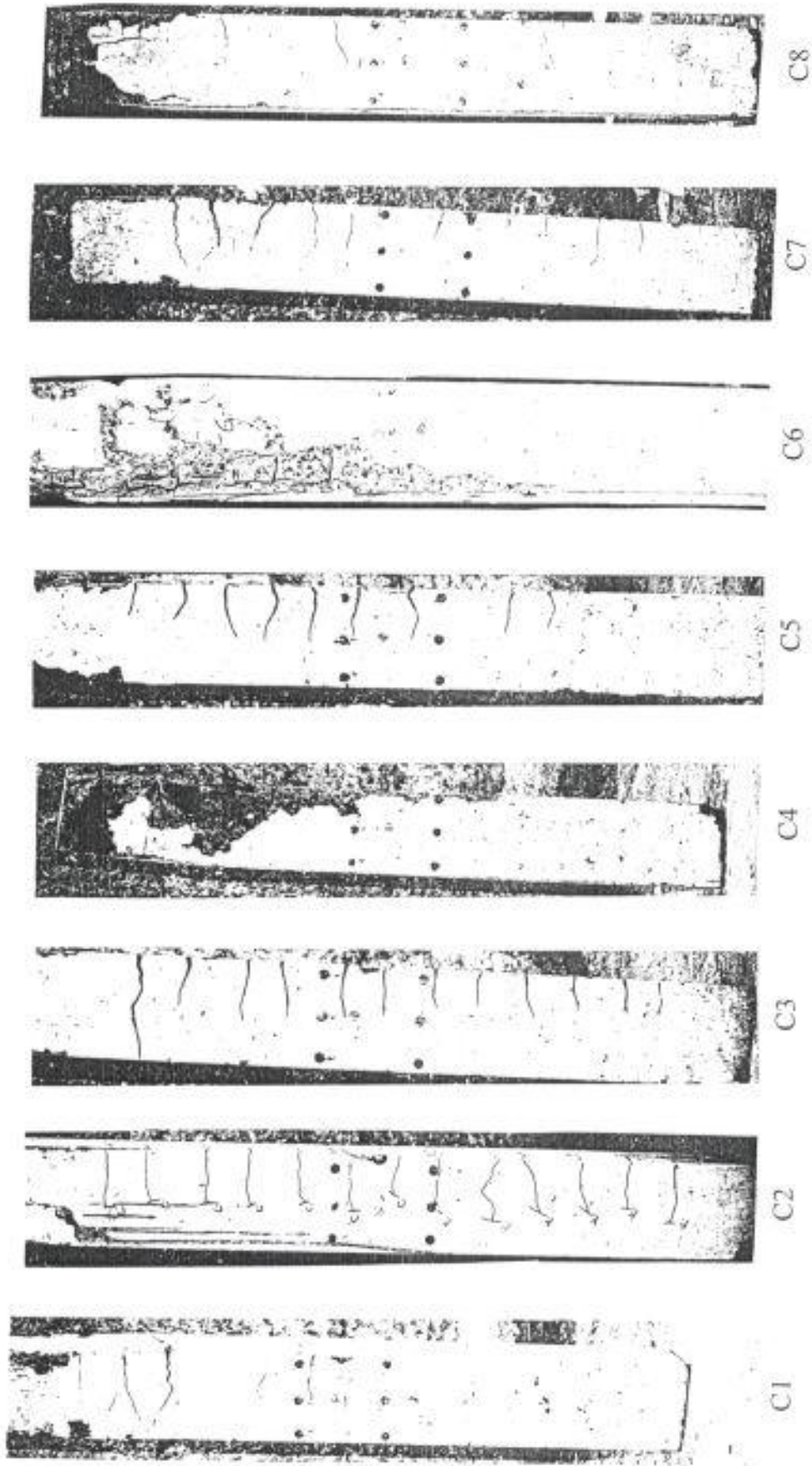


Figure 5 Crack patterns for studied column specimens.

## 4.1.2 Load Displacement Relationship

The effects of the studied parameters on the relation between the ultimate measured load capacity and the corresponding lateral displacement are illustrated in Figure 6 through Figure 8 and discussed in the following sections.

### 4.1.2.1 Effect of load eccentricity

Figure 6 shows that increasing load eccentricity resulted in reducing the expected ultimate capacity of the studied columns. For example, increasing the eccentricity ratio ( $e/t$ ) from 0.21 for the column "C1" to 0.42 for the column "C2" lead to a reduction of the ultimate load of approximately 15%. In addition, the slope of the load-mid-height lateral displacement curve was reduced from 17.4 t/mm to 6.25 t/mm for the columns "C1" and "C2", respectively. It was observed also that NSC Column "C4" had the lowest column capacity and slope of the curve compared with those of HSC columns. The ultimate capacity and slope of the curve for Column "C4" were approximately 56% and 32% of that for Column "C1", respectively. It can be seen from Figure 6 that the maximum displacement of the studied columns increased with the increase of load eccentricity. For example, increasing the eccentricity ratio ( $e/t$ ) from 0.21 for Column "C1" to 0.42 for Column "C2" resulted in increasing the lateral displacement by 112%. For the same load eccentricity ratio, NSC Column "C4" exhibited a larger displacement than that of HSC one "C1" by approximately 50%. The area under the curve for columns "C4" and "C1" was about 211 and 252.5 t.mm, respectively. This assures the ductility of HSC confined columns as stated earlier by Foster and Attard[1].

### 4.1.2.2 Effect of transverse steel

Figure 7 shows the effect of both transverse (lateral) steel ratio and configuration type on the load displacement relationship. It can be seen that increasing the lateral confinement of columns "C5", "C6", and "C7" lead to an increase of both ultimate capacity and lateral displacement over Column "C1" by approximately 21.8% and 127.4%, respectively. In addition, the ultimate capacity for columns "C6" and "C7"

was greater than that of Column "C5" by 13% and 8.3%, respectively. This indicates that the presence of cross ties for column stirrups was more efficient than decreasing the spacing between stirrups. The area under the curve, for columns "C5", "C6" and "C7", was approximately triple that for Column "C1". This confirms the earlier findings of the efficiency of the lateral steel and its influence on the ductility of HSC columns [1, 15 and 16].

#### **4.1.2.3 Effect of longitudinal reinforcement**

The effect of longitudinal reinforcement on the load displacement relationship is shown in Figure 8. Increasing the longitudinal steel ratio by approximately 43 % for Column "C8" lead to an increase in the ultimate column capacity by 19% and the maximum lateral displacement by 74% compared with those of Column "C1". In addition, the area under the curve for Column "C8" was increased by approximately 75% with the increase of longitudinal steel ratio compared with that of Column "C1". This indicates that increasing longitudinal steel ratio improved the ductility of studied HSC columns. It is worth mentioning that the area under the curve for Column "C8" is almost double as much of that for Column "C4", which shows that the Studied HSC columns are more ductile than the NSC one.

#### **4.1.3 Concrete Strains**

Figure 9 presents the concrete strain distribution across the section at mid-height of all test columns at half of the maximum loads (prior to cracking) and at maximum loads. The figure shows that increasing the lateral steel confinement and decreasing the spacing between ties increased the ultimate concrete compressive strain for HSC columns. For example, Columns "C5", "C6", and "C7" had ultimate compressive strain higher than that of Column "C1" by a range of 16-78%. In addition, providing cross ties for column stirrups was more effective in increasing concrete compressive strain than decreasing the spacing between stirrups. For example, the compressive strain of Column "C5" was higher than that of Column "C1" by 34% while that of



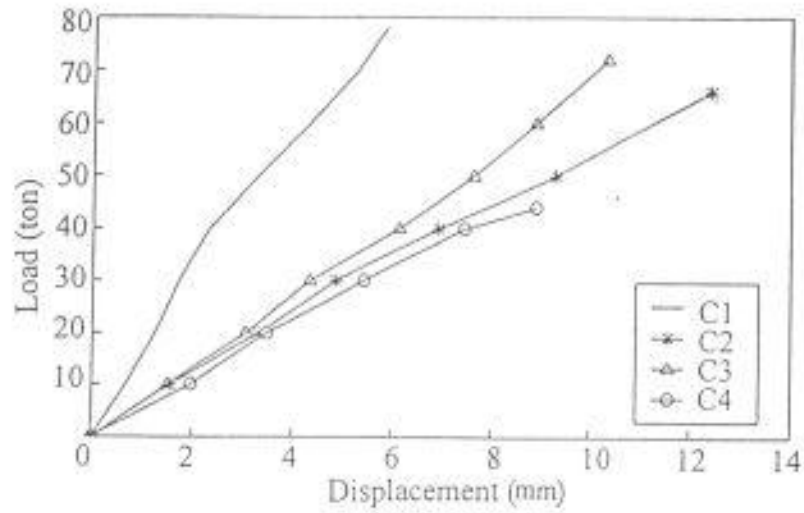


Figure 6 Effect of load eccentricity on the load-displacement relationship.

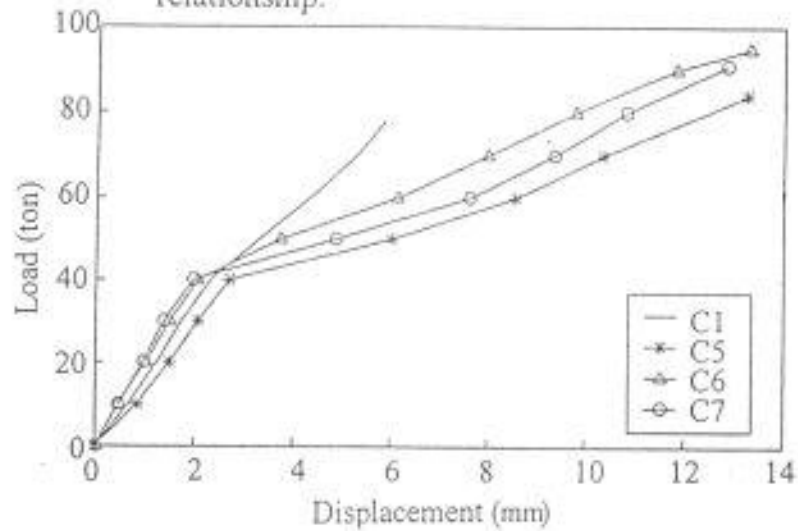


Figure 7 Effect of transverse steel ratio and type on the load-displacement relationship.

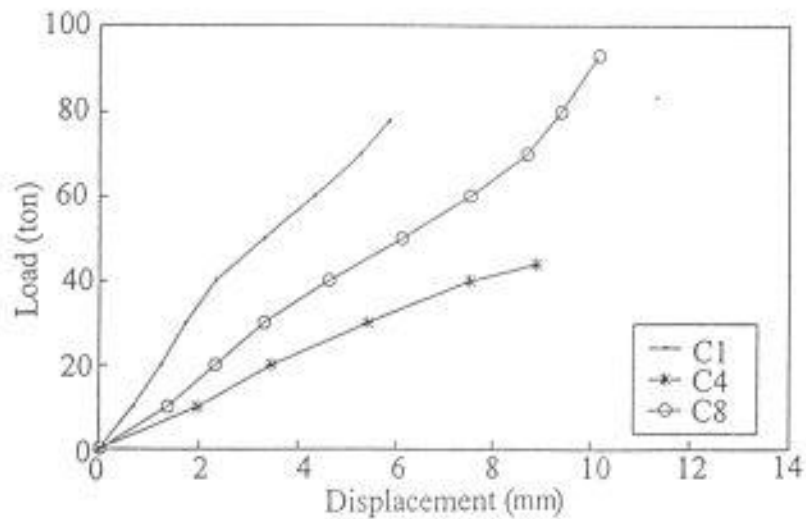


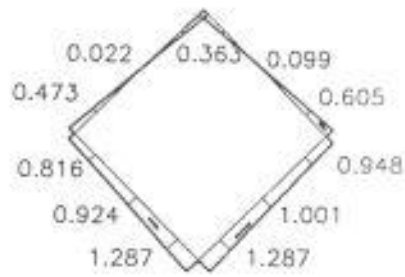
Figure 8 Effect of longitudinal reinforcement on the load-displacement relationship.

Column "C6" was higher than that of Column "C1" by 78%. It can be seen from Figure 9 that the effect of increasing confinement on the compressive strain at half of the maximum load (before cracking) was not significant.

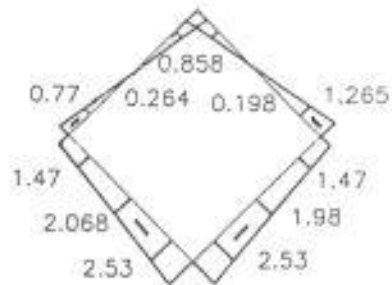
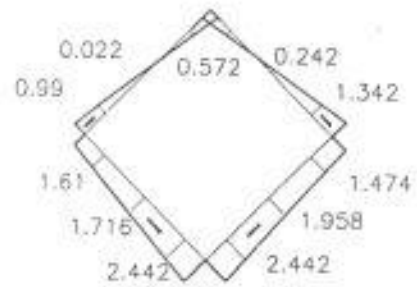
Figure 9 shows also that the maximum compressive strain increased as the longitudinal reinforcement ratio increased. For example, the compressive strain of Column "C8", at maximum load, was higher than that of Column "C1" by approximately 32%. On the other hand, despite that the load eccentricity was highly effective on the compressive concrete strain before cracking (at half of the maximum load), it was found that such effect reduced at maximum load (after cracking). For example, the compressive strain of Column "C2" was higher than that for Column "C1" by 102% at half of the maximum loads while it was higher by 4% only at maximum load (after cracking). In addition, the compressive strain of Column "C3" was higher than that for Column "C1" by 66 % at half of the maximum loads while it was higher by 58% at maximum load.

#### 4. 2 Analytical Results

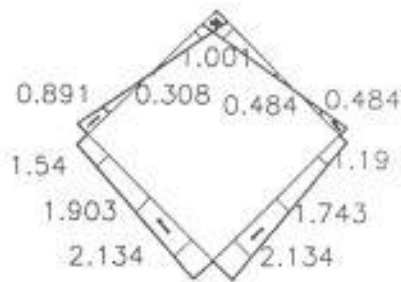
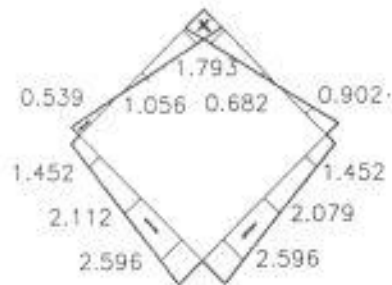
The estimated ultimate capacities for the columns, using the charts produced by the computer program developed earlier [10], are listed in Table 3, as well as the measured experimental values and those predicted by the proposed design formula, Equation (7) at Section 3.3. Table 3 shows that the values calculated by the charts and those obtained by the proposed formula underestimate the columns' capacities, or in other words, are conservative estimates. As a result of ignoring the effect of lateral confinement in the calculation using the charts, theoretical capacities of Columns "C5", "C6" and "C7" were almost the same with minor variations attributed to the difference of actual concrete compressive strength of each column. On the other hand, taking the effects of confinement and eccentricities into consideration in the proposed formula was significant in predicting the capacities of Columns "C5", "C6" and "C7" as shown in Table 3. It can be noticed that the proposed formula is simple and fast. However, it needs to be verified by more experimental work in future.



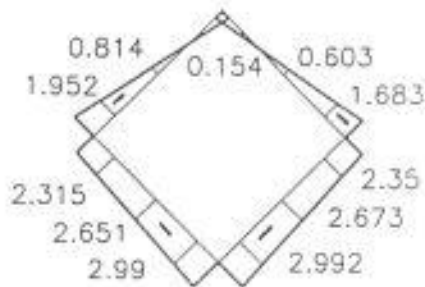
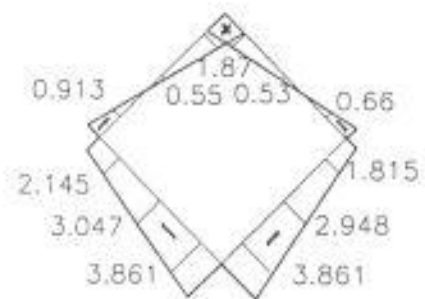
Col. C1



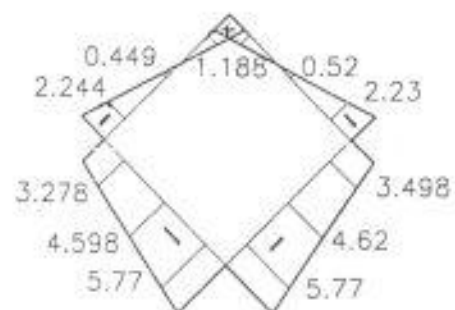
Col. C2



Col. C3



Col. C4

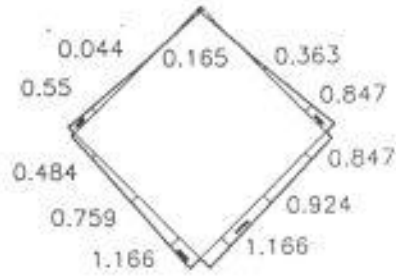


$$P = \frac{1}{2} P_{max}$$

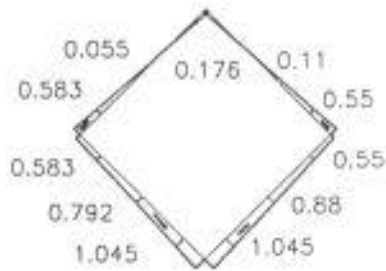
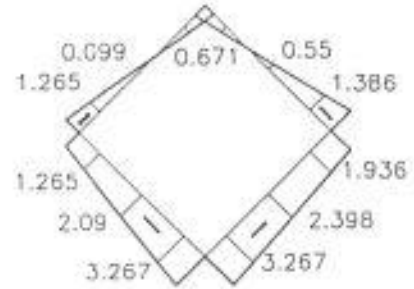
$$P = P_{max}$$

(Strain x 0.001)

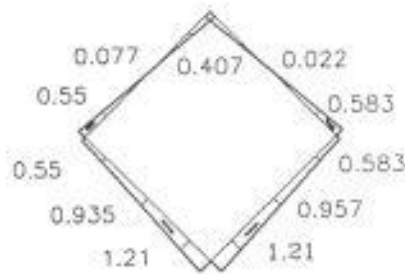
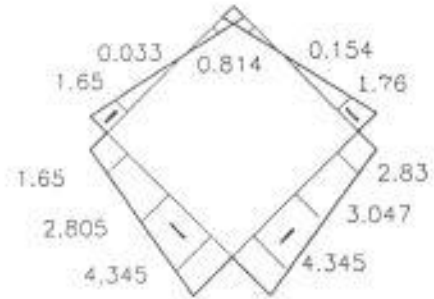
Figure 9 Concrete strain distribution across the section for studied columns.



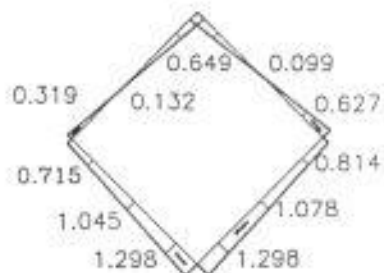
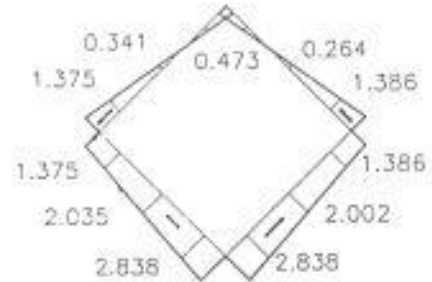
Col. C5



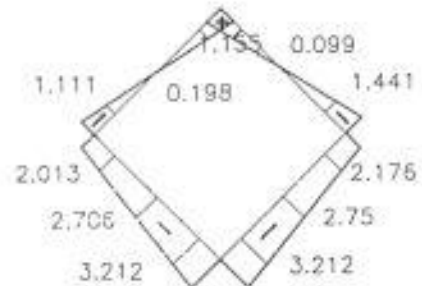
Col. C6



Col. C7



Col. C8



$$P = \frac{1}{2} P_{max}$$

(Strain x 0.001)

$$P = P_{max}$$

Figure 9 (Continued) Concrete strain distribution across the section for studied columns.

Table 3 Experimental and Theoretical Ultimate Capacity of Studied Columns

Column Specimen Number	Concrete Strength, $f_{cu}$ (kg/cm <sup>2</sup> )	Experimental Load Capacity, $P_{Exp}$ (ton)	Predicted Load Capacity			
			$P_{th}^*$ (ton)	Error, %	$P_{max}^{\#}$ (ton)	Error, %
C1	748	78	62	20.5	69	11.5
C2	762	68	40	39.4	66	3.0
C3	735	72	50	30.6	66	8.3
C4	386	44	39	11.4	42	5.0
C5	782	86	72	14.3	85	1.1
C6	782	95	76	20	74	22
C7	790	91	74	18.7	75	18.0
C8	734	93	78	16.1	78	16.1

\* calculated capacity using computer program [10].

# calculated capacity based on proposed formula, Equation (7).

## 5. CONCLUSIONS

Based on the experimental and theoretical results in this paper, the following conclusions can be drawn:

1. Increasing load eccentricity resulted in reducing the ultimate capacity of the studied columns by approximately 15% and increasing the maximum lateral displacement by approximately 112%. Despite that the load eccentricity was highly effective on the compressive concrete strain before cracking (at half of the maximum load), it was found that such effect was reduced at maximum load (after cracking).
2. Increasing the lateral confinement leads to an increase of ultimate capacity and lateral displacement by approximately 21.8% and 127.4%, respectively. Ultimate compressive strain was increased by a range of 16-78%. The presence of cross ties for column stirrups was more efficient than decreasing the spacing between stirrups in improving the ductility of the studied HSC columns.



3. The increase of longitudinal steel ratio resulted in an increase of the ultimate column capacity, the maximum lateral displacement and the ultimate compressive strain. This is an indication of improving the ductility of such HSC columns.
4. Within the limits of the test results of this study, the proposed design formula shows a reasonable accuracy since it predicts the columns' capacities with an average error of 11% only taking the effects of confinement and eccentricities into consideration. However, it needs more verification in order to be used as a good preliminary estimate of HSC column's capacity.

## 6. REFERENCES

1. Foster, S. J and Attard, M. M, "Experimental Tests on Eccentrically Loaded High-Strength Concrete Columns", ACI Structural Journal, Vol. 94, No. 3, pp. 295-303, May-June 1997.
2. ACI - ASCE Committee 441, "High-Strength Concrete Columns: State of the Art", Committee Report, ACI Structural Journal, Vol. 94, No. 3, pp. 323-335, May-June 1997.
3. Ibrahim, H. H and MacGregor, J. G., "Tests of Eccentrically Loaded High - Strength Concrete Columns", ACI Structural Journal, Vol. 93, No. 5, pp. 585-594, September - October, 1996.
4. ACI Committee 363, "State-of-the-Art Report on High Strength Concrete", ACI 363R-92, American Concrete Institute, Box 19150, Redford Station, Detroit, Michigan, 55 pp, September 1992.
5. Claeson, C. and Gylltoft, K., "Slender Concrete Columns Subjected to Sustained and Short-Term Eccentric Loading," ACI Structural Journal, Vol. 97, No. 1, pp. 45-52, January-February 2000.
6. Lee, J. and Son, H., "Failure and Strength of High-Strength Concrete Columns Subjected to Eccentric Loads", ACI Structural Journal, Vol. 97, No. 1, pp. 75-85, January-February 2000.
7. Legeron, F. and Paultre, P., "Behavior of High-Strength Concrete Columns under Cyclic Flexure and Constant Axial Load", ACI Structural Journal, Vol. 97, No. 4, pp. 591-601, July-August 2000.
8. "Egyptian Code for the Design and Construction of Reinforced Concrete Structures", Cairo, 1995.
9. El-Sayad, H. I. And El-Dash, K. M., "Concrete Confined Externally by Pre-Stressed Steel Straps," CERM, Vol. 21, No. 1, pp. 159-175, January 1999.

10. El-Mihilmy, M. T., "Behavior and Design of R.C. Short Columns under Biaxial Bending", M.Sc Thesis submitted to Cairo University, 333pp, 1992.
11. Collins, M. P., Mitchell, D. and MacGregor, J. G., "Structural Design Considerations for High Strength Concrete," Concrete International, Vol. 15, No. 5, pp. 27-34, May 1993.
12. Liu, J., Foster, S. and Attard, M., "Strength of Tied High-Strength Concrete Columns Loaded in Concentric Compression", ACI Structural Journal, Vol. 97, No. 1, pp. 149-156, January-February 2000.
13. Sheikh, S. A., and Uzmeri, S. M., "Analytical Model for Concrete Confinement in Tied Columns," Journal of Structural Engineering, ASCE, Vol. 108, No. 12, pp. 2703-2722, 1982.
14. Mander, M. J., Priestley, M. J. N.; and Park, R., "Theoretical Stress-Strain Model for Confined Concrete, Journal of Structural Engineering, ASCE, Vol. 114, No. 8, pp. 1804-1826, August 1988.
15. Bing, L., Park, R. and Tanaka, H., "Constitutive Behavior of High-Strength Concrete under Dynamic Loads," ACI Structural Journal, Vol. 97, No. 4, pp. 619-629, July-August 2000.
16. El-Nesr, O., "Confining Effect on the Ductility Behavior of Reinforced Concrete Columns," The Eighth Arab Structural Conference Proceedings, Vol. 2, pp. 615-622, 21-23 October 2000.

### مطولية الأعمدة الخرسانية المسلحة عالية المقاومة والمعرضة لقوى ضغط مع عزم مزدوج

#### ملخص:

يتضمن البحث صب واختبار عدد ثمانية أعمدة خرسانية مسلحة عالية المقاومة ذات قطاع 150 مم x 150 مم وارتفاع 1200 مم وذلك بغرض دراسة سلوك تلك الأعمدة تحت تأثير أحمال لامركزية في الاتجاهين. واشتمل البحث على دراسة تأثير عدد من المتغيرات منها نسبة اللامركزية للحمل في الاتجاهين س، ص؛ نسبة التسليح العرضي (الكانات) وكذلك شكلها بالإضافة الى نسبة التسليح الطولي للأعمدة. وقد أظهرت نتائج الدراسة أن زيادة نسبة لامركزية الحمل في كلا الاتجاهين تؤدي الى نقص المقاومة القصوى للأعمدة بحوالي 15%؛ وزيادة نسبة التسليح العرضي تؤدي الى زيادة المقاومة القصوى للأعمدة بحوالي 22% وكذلك زيادة نسبة التسليح الطولي تحسن من مطولية الأعمدة. كما أظهرت النتائج مدى فاعلية شكل الكانات في تحسين مطولية الأعمدة الخرسانية المسلحة عالية المقاومة. وأخيراً تم اقتراح معادلة افتراضية للاستعانة بها في تصميم مثل هذه الأعمدة وقد أظهرت المقارنة الأولية تقارب نتائجها مع نتائج الاختبارات المعملية.